7th International Conference on Innovation in
SCIENCE AND TECHNOLOGY
23 - 25 October, 2020 Amsterdam, Netherlands

Applying Reduced Graphene Oxide-Gold Nanoparticles for the Electrochemical Detection of Endotoxin

Fatemeh Yazdian[1*], Hamid Rashedi[2*]

[1] Department of Life Science Engineering, Faculty of New Science and Technologies, University of Tehran, Tehran, Iran

[2] School of Chemical Engineering, College of Engineering, University of Tehran, Tehran, Iran

*Corresponding authors:

yazdian@ut.ac.ir

hrashedi@ut.ac.ir

Abstract.

The outer membrane of gram-negative bacteria releases lipopolysaccharides (LPS) or endotoxins that make toxic effects on humans. Therefore, the selective detection and sensitivity of LPS is so vital especially in the field of therapeutics, medical supplies, and in the food industry. In this study, in order to detection of LPS an ultrasensitive electrochemical biosensor was fabricated through the immobilization of endotoxin-specific thiolated aptamer on the surface of reduced graphene oxide-gold nanoparticles (rGO-Au NPs) modified electrode. The biosensor is found to detect the small amounts of LPS in 35 minutes and was able to distinguish the endotoxin molecules from the interfering biomolecules such as bovine serum albumin, fetal bovine serum, and glucose. Hence, this sensor has excellent sensitivity and selectivity toward LPS, in spite of its convenient and easy construction procedure. the Real sample test proved that patient group has higher ΔI (higher than 55 mA) comparing with the normal group (less than 55 mA).

Keywords: Endotoxin; Aptasensor; Gold nanoparticles; Lipopolysaccharide; Methylene blue

1. Introduction

Lipopolysaccharide or endotoxin is the main part of the outer membrane of a gram-negative bacterium, which gives an appropriate resistance to the bacterial membrane, as it can tolerate high temperature intrinsically. This macromolecule consists of three main parts named as O-specific antigen on top, core polysaccharide, and a non-polar region called lipid A at the most inner part (Ding et al., 2015; Posha & Sandhyarani, 2020). Endotoxins are responsible for the toxic effects that cause septic shock, fevers, and sepsis (Ji et al., 2020). They have the means for attaching to other molecules. Some examples are lectins and some enzymes involved in endotoxin degradation like lysosomal phosphatase and granule acyloxyacyl hydrolase, which could be recognized by the O antigen of the endotoxin (P.

Miao, 2013). While lipopolysaccharides are attached to the bacterial membrane, they can be released into the environment where the bacterium is present. This can happen during the cell-growth, -division, -death, or treatment with antibiotics (Das et al., 2014). By being liberated into the bloodstream, endotoxins cause severe health issues, such as fever, septic shock, respiratory problems, multi-organ functional disorders, and even neurological disorders like Alzheimer (Glauser & Zanetti, 1991; Schwartz et al., 1995; Zhao et al., 2017). Many people with different jobs and lifestyles are exposed to endotoxins as these molecules are present in almost all kinds of environments and workplaces, namely agricultural fields, poultry farms, slaughterhouses, waste collection areas, furniture manufacturing factories, textile industry and so on (Liebers et al., 2006). Food and drug administration (FDA) has set limits to the concentration of LPS, such as 0.5 $EU.mL^{-1}$ (Endotoxin Unit, 1 EU=0.1 ng) for medical devices, 0.06 $EU.mL^{-1}$ (1 EU ≈100pM) for devices in contact with cerebrospinal fluid, and 0.2 $EU.kg^{-1}.hr^{-1}$ for intrathecal drugs (Su, Cho, et al., 2013). Consequently, it is very important to control the amount of LPS in different pharmaceutical and food products. There are various methods for the detection of endotoxin in a sample, among which culture-based methods, which rely on the relationship between the number of bacteria and the concentration of LPS have some disadvantages. For instance, each strain needs its fresh specific culture media and optimal condition plus many days of incubation to show a positive result. Rabbit pyrogen test and LAL (Limulus amebocytes lysate), the second one being more sensitive and common, are other quantitative detection methods. However, these techniques are time consuming, laborious and have low reproducibility (Park et al., 2005).

The drawbacks to the mentioned approaches for LPS detection are good reasons to shift into the new ones that demand less time and effort. Biosensors are relatively new methods for LPS sensing that are mainly categorized into three groups of optical-, mass-, and electrochemical-based sensors. Each of these methods has its pros and cons. Regarding sensitivity, optical biosensors seem to be more advantageous, but they are mostly economically unaffordable. Mass-based biosensors, however, are not that costly but lack appropriate sensitivity and selectivity (Law et al., 2014). The electrochemical type, on the other hand, is easier to be commercialized due to its reasonable cost and shows acceptable performance characteristics like high reproducibility, sensitivity, and stability. Kim et al. 2012 constructed one of the first electrochemical biosensors that could detect LPS at the appropriate range of 0.01-1 $ng.ml^{-1}$ and had the potential to replace the older methods for detection of this macromolecule (Kim et al., 2012). With the same intention, some newer research has been done to improve the detection procedure with the aid of electrochemical biosensors by integrating novel nanocomposites and recognition agents into the sensor's structure (Bai et al., 2014; Su, Cho, et al., 2013; Zuzuarregui et al., 2015).

Among different nanomaterials, the fascinating properties of graphene, as a carbon-based nanomaterial, such as high surface area, optical and magnetic properties, electrical and thermal conductivity, and high elasticity, makes it an appropriate base structure for preparing a number of graphene-based nanocomposites, especially as a great candidate to be used in a biosensor structure (Geim & Novoselov, 2007; Lee et al., 2008). Even though graphene has many favorable properties for being used in sensors, lack of functional groups makes it hard to immobilize recognition biomolecules on it. With this in mind, different derivatives of graphene, named as graphene oxide (GO) and reduced graphene oxide (rGO) are being used

in biosensors' structures. GO, with its carboxyl groups on the edges and epoxy groups on its basal plane, has the possibility of attaching to biomolecules (Gao, 2015). Moreover, by applying a reduction process on this material, another derivative of graphene, reduced graphene oxide (rGO), is produced. reduced graphene oxide (rGO) not only has the advantage of remaining the carboxyl groups after the reduction process, but also has a better charge transfer ability due to losing of epoxy and hydroxyl groups as well as having defects in its structure (Sanguansak et al., 2014). These optimal properties of rGO have made it become a suitable nanomaterial used in many biosensors for the detection of microorganisms or their toxins (Vanegas et al., 2015; Wu & Chai, 2017; Xu et al., 2016; Zhang et al., 2017). Using rGO, Krittayavathanano et al. 2017 were able to quantify aflatoxin B1 down to 0.04 $ng.ml^{-1}$. In their study, a single strand DNA immobilized on rGO was assembled on a rotating disk electrode to reduce the charge transfer resistance by increasing rotating speeds (Krittayavathananon & Sawangphruk, 2017).

Using other materials in composition with graphene is one good way to increase its novel properties. Metal nanoparticles such as Au-, Pt-, Pd-, Ag- and Li-nanoparticles, as well as their oxide and sulfide compounds, are frequently being used in combination with graphene to form a favorable nanocomposite to be used in different types of biosensors (Bai et al., 2014). Due to their free electrons, metal nanoparticles can absorb visible and ultraviolet light and therefore are applicative in many optical biosensors using surface plasmon resonance effect (Wang et al., 2018). The decent catalytic properties of metal nanoparticles make them suitable for electrochemical biosensors as well (Luo et al., 2006). Moreover, high surface area, high mechanical strength, and electrostatic adsorption of biomolecules are general properties of metal nanoparticles such as gold nanoparticle to improve conductivity and used as a bed for immobilization of bio receptors (Pourmadadi et al., 2020), that are beneficial to the biosensor structure (Doria et al., 2012). Govindhan et al. 2015 showed that Au-rGO/GCE makes a bigger anodic peak in the cyclic voltammograms in contrast to both Au/GCE and rGO/GCE approving that these two have a better electrochemical feature in collaboration with each other (Govindhan et al., 2015). Yuan et al. 2019 fabricated an electrochemical sensor for LPS detection in which they used a metal sulfide (MoS_2) in a graphene-based nanocomposite and also utilized a metal nanoparticle (AuNPs) for immobilization of the detecting aptamer. In both cases adding metal materials led to increasing of electrochemical signals (Yuan et al., 2019).

Nucleic acids, peptides, proteins, antibodies, and phages are more or less used as biorecognition elements to detect microorganisms or their products. Among all, aptamers, which are single strand DNA or RNA with 15 to 40 nucleotides, have been showing a great affinity toward their target analytes. Aptamers have some advantages over other biomolecules, such as having a wide range of target molecules from amino acids to different proteins and even a whole cell, being affordable, having a small size, having a reversible denaturation and remaining their chemical properties in different buffers (Mairal et al., 2008). Su et al. 2012 fabricated a biosensor by modifying Au-electrode with 3-mercaptopropionic acid (MPA) as a linker to attach amine terminated single strand DNA aptamer on it. The obtained linear range is reported as 0.001-1 $ng.ml^{-1}$ (Su et al., 2012). Posha et al. 2017 modified a gold electrode with the gold atomic cluster to immobilize an aminated aptamer on

it and constructed a biosensor, which had the detection limit of 7.94×10^{-21} M (Posha et al., 2018).

Methylene blue (MB) is a biological stain and redox indicator, with an excellent affinity toward single strand DNA oligonucleotides. The stronger affinity of MB toward ssDNA compared to its weaker affinity toward dsDNA along with its electron transfer ability makes it a good hybridization indicator. Erdem et al. 2000 designed an electrochemical biosensor for the detection of a DNA sequence related to hepatitis B virus. In their study a probe specific to this DNA sequence, was immobilized on the electrode. The hybridization process could be tracked via measuring decline in voltametric signals of methylene blue after being replaced by viral DNA on the electrode surface (Erdem et al., 2000). Using another approach, Zejli et al. 2019 used methylene blue tagged aptamer for detection of Aflatoxin B1. In their study the modification in aptamer's conformation after binding with toxin led to more MB species being nearby the surface of electrode and thereby a greater current response in differential pulse voltammetry (DPV) analysis (Zejli et al., 2019).

In this study, we present a highly sensitive electrochemical aptasensor, fabricated with the aid of reduced graphene oxide and gold nanoparticles, for the detection of LPS. For the first time among all experiments done so far, through immersing the electrode in methylene blue, we were able to accumulate MB species on the electrode via their attachment to the single strands of DNA (aptamers) and measure the charge transfer process, which is mediated by MB (250 mM) redox couples in PBS buffer. This improved the electrodes performance significantly and brought the LOD of our biosensor down to femtomolar level. Finally, the real sample was test and results were achieved.

2. Materials and Experimental Methods

2.1 Materials

Graphite powder, Sulfuric acid (98 wt%), Chloroauric acid, Sodium permanganate, K3Fe (CN)6, Hydrogen peroxide, Sodium Borohydrate, and Ethanol were purchased from Merck (Germany). Phosphate buffered solutions (PBS, ten mM, pH 7.4) containing NaH2PO4, and Na2HPO4 were purchased from Amertat Company (Tehran, Iran). The aminated aptamer 5'–NH2–(CH2)6CTTCTGCCCGCCTCCTTCCTAGCCGGATCGCGCTGGCCAGATGATATAAAGGGTCAGCCCCCCAGGAGACGAGATAGGCGGACACT-3' was purchased from Biobasic (Canada) and stored at -20 °C before use. 1-ethyl-3- (3-dimethylaminopropyl) carbodiimide (EDC), N-dimethylformamide (DMF), Nafion (0.1 %wt), LPS from Escherichia coli 055:B5 (L2880), and Glucose were purchased from Sigma-Aldrich. Bovine serum albumin (BSA) and fetal bovine serum (FBS) were purchased from Equitech-Bio (USA). Methylene blue (MB) was purchased from Merck (Germany). All solutions were prepared with deionized distilled water, which was purified by the water purification system of the CRI Company (Iran). Hydrogen peroxide was purchased from Merck (Germany).

2.2 Instrumentation

Cyclic voltammetry (CV), differential pulse voltammetry (DPV), electrochemical impedance spectroscopy (EIS), and squarewave voltammetry (SWV) were performed using Ivium vertex Potentiostat/Galvanostat (Ivium Technologies), and the resulting data were recorded with IviumSoft™ Electrochemistry *software*. All these electrochemical experiments were carried out in a three-electrode system consisting of a platinum counter electrode, a Ag/AgCl as a reference electrode, and a glassy carbon electrode with the diameter of 2mm as working electrode (NARSElab, Iran). EIS measurements were performed with 0.01 mV amplitude sine wave, and in the frequency range of 0.01 Hz to 100000 Hz. The morphology was imaged and studied by transmission electron microscopy (TEM) on Zeiss-EM90C instrument with an accelerating voltage of 100 kV. The identification of crystalline samples was carried out by x-ray diffraction (XRD) with Philips diffractometer. Fourier transform infrared spectroscopy (FTIR) was performed for structural characterization of synthesized nanocomposites using Shimadzu infrared spectrometer.

2.3 Synthesis of rGO-AuNPs

In order to synthesize the graphene oxide, the modified Hummers' method was used (Akbari jonous et al., 2019; Pourmadadi et al., 2019, 2020; Shahriary & Athawale, 2014). Firstly, 1 g of graphite powder was added to 20 ml of sulfuric acid 98% and was stirred in an ice bath which was placed on a mechanical stirrer. After 30 minutes, 3 g of sodium permanganate was slowly added to this solution and gradually turned the color of the solution to slime green. After another 30 minutes, 50 ml of distilled water was slowly dropped into the solution followed by adding another 100 ml of distilled water after ten minutes. 30 minutes later, 35 ml of Hydrogen peroxide was added and this final solution stayed on the magnetic stirrer with heater for 24 hours. This graphene oxide was added to 100 ml distilled water and sonicated until being homogenous. Next, 1 g of sodium borohydride was slowly added to the mixture, followed by drying under 100 Cº for 24 hours. Further, ethanol and water in a ratio of 1:1 were added to the dried powder and centrifugation was carried out. The precipitant was placed in a vacuum oven at 80 Cº for 24 hours subsequently to obtain a reduced graphene oxide powder. After that, 0.35 of this powder was dissolved in 80 ml of distilled water and ultrasonicated for ten minutes. Afterward, 2 ml of HAuCl4 (25% M) was added gradually, and the mixture was stirred on a stirrer at room temperature for 3 hours. After evaporation of the liquid part, the precipitate is collected and washed with water and ethanol by centrifuge and dried with a freeze dryer. The final product was reduced graphene oxide-Au nanoparticles, which would be used for the fabrication of the modified electrode.

2.4 Fabrication of rGO-Au NPs-Apt modified electrode

To obtain a stock from the lyophilized aptamer, 62 µL of sterile water was added to this powder, and the mixture was divided into 16 volumes of 2 µL, one volume of 20 µL, and one volume of 10 µL subsequently, which were all stored at -20 °C for future usage. In order to add aptamers to the previously synthesized reduced graphene oxide-Au nanoparticles composite, we used 5-Ethynyl-2'-deoxycytidine (EDC) and N-Hydroxysuccinimide (NHS) as crosslinkers. Linkers activate the amine end of the aptamers, and consequently facilitate the formation of amide bonds between carboxyl groups of the rGO-Au NPs and

amine_terminated aptamers. With this intention, 100 µL of EDC was mixed with 100 µL of NHS and were shaken together for ten minutes. After that, 200 µL of the prepared reduced graphene oxide-gold nanoparticles nanocomposite with the concentration of 0.25 mg.mL-1 was added and shaken for 15 minutes. Further, this mixture was added to the volume of 2 µL of aptamer and shaken for about 3 hours. After another shake at the rate of 3.8 rpm for two minutes, the upper suspension was removed with the aid of a sampler without disturbing the precipitates. These precipitates were then vortexed to be homogeneous, and 20 µL of this was added to 2 µL volume of nafion with the concentration of 0.1 v/v. In order to find the optimum volume of nafion to be added to the graphene oxide-gold-aptamer mixture, three ratios of reduced graphene oxide:nafion (1:6, 1:8, and 1:10) mixtures were prepared and compared with each other in cyclic voltammetry mode. Finally, the ratio of 1:10 was observed to have the highest peak current and was selected to be added to the mixture. The addition of nafion was followed by 15 minutes of incubation in the room temperature.

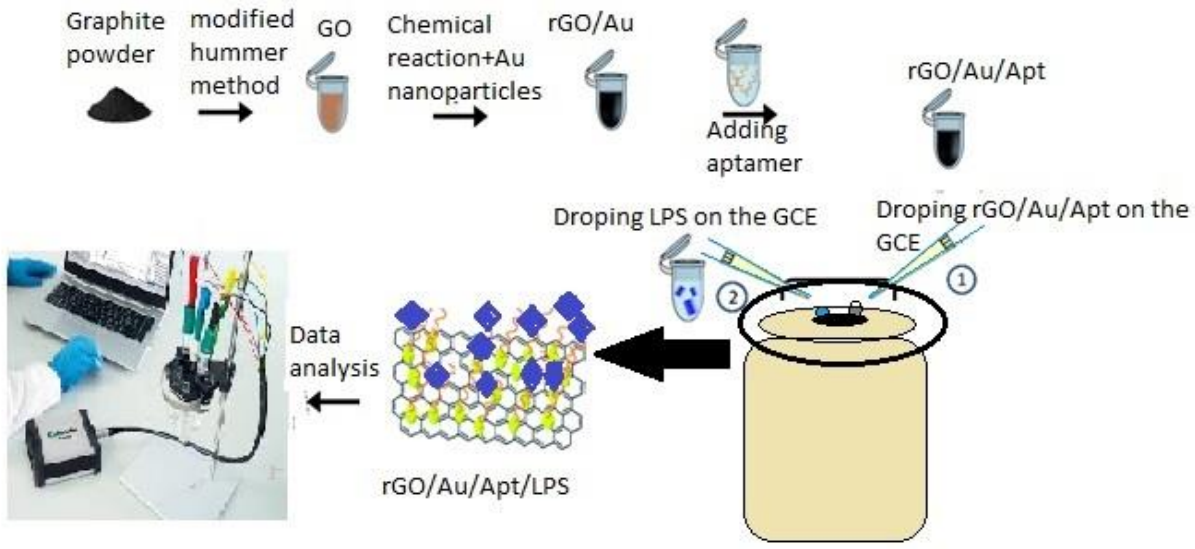

Scheme 1: Schematic representation of the fabrication procedure of the rGO/Au/Apt sensor.

2.5 Real Sample Analysis

Four serum samples including two positive control (patient sample) and two negative control (normal sample) samples determined by E-TOXATE (The E-TOXATE (Limulus Amebocyte Lysate) test kits purchased from Sigma-Aldrich that is intended for semiquantitative detection of endotoxins for research purposes were used. Both real patient and normal samples were diluted 100, 300, 500, 700, and 900 times to prevent the effect of confounding factors and placed 10 µL of the lowest concentration of real samples as analyte on the electrode surface, followed by incubation with specific aptamer for 35 min as same as synthetic samples protocol. Then washed by addition PBS with pH =7.4 to remove unbound lipopolysaccharide similarly for subsequent concentrations of low to high concentrations for all 4 real negative control and positive control samples.

3. Results and discussion

3.1 Characteristics of synthesized nanomaterials

Figure 1 presents the x-ray diffraction (XRD) spectra of GO and RGO/AuNPs samples. As displayed in **Error! Reference source not found.** the XRD pattern of GO had an intense diffraction peak centered at 2Θ=9.91º correspondsto the (001) interplanar distance of 0.89 nm, which shows the proper oxidation of graphite to graphene oxide and an increase in interlayer spacing. The existence of a very weak and broad peak (002) in the XRD spectrum of GO is assumable due to the presence of some stacking of graphite in the sample. Moreover, the XRD pattern of rGO-Au NPs indicates diffraction peaks at 2Θ=38.14º, 44.32º, 64.66º, and 77.74º which are corresponding to (111), (200), (220), and (311) crystalline planes of Au. Also, the (001) peak of GO is disappeared specifying the reduction of GO. Furthermore, a broad diffraction peak at 2Θ=15-30 indicates disordered reduced graphene oxide sheets (Pourmadadi et al., 2019, 2020).

FTIR spectra of the GO, rGO-Au NPs, and rGr-Au NPs-Apt is depicted in Figure 1b. From the GO spectrum, the absorption peak at 1050 cm-1 and 1220 cm-1 attribute to C-O alkoxy stretching vibration and C-O epoxy stretching vibration respectively. At 1410 cm-1 there is a small peak, which is associated with the OH deformation vibration. The peak at 1710 cm-1 is related to C=O functional groups. The intense and wide peak from 2880 to 3650 corresponds to O-H stretching vibration. The existence of oxygen-containing functional groups demonstrates the proper oxidation process applied to primary graphite powder. The peak at 1600 cm-1 is assigned to the C=C bonds, which are present before and after oxidation. In rGO-Au spectrum the O-H stretching vibration is found to become less intense, which could be due to their attachment with metal ions via electrostatic interactions. The attachment of aminated aptamers to the synthesized nanocomposite took place using EDC/NHS crosslinking, wherein NHS ester groups and the terminal –NH2 groups of the aptamers were covalently linked together. This attachment is exhibited in the GO-Au NPs-Apt spectrum as the (C-NH-C) bending peak at 1200 cm^{-1} (Pourmadadi et al., 2019, 2020).

Transmission electron microscopy (TEM) of the rGO-Au NPs is shown in Figure 1. The uniform distribution of rounded and faceted shape Au-NPs on the rGO sheets is clear in the TEM images, indicating that the dispersion of these particles on the nanomaterial was successful and agglomeration did not happen.

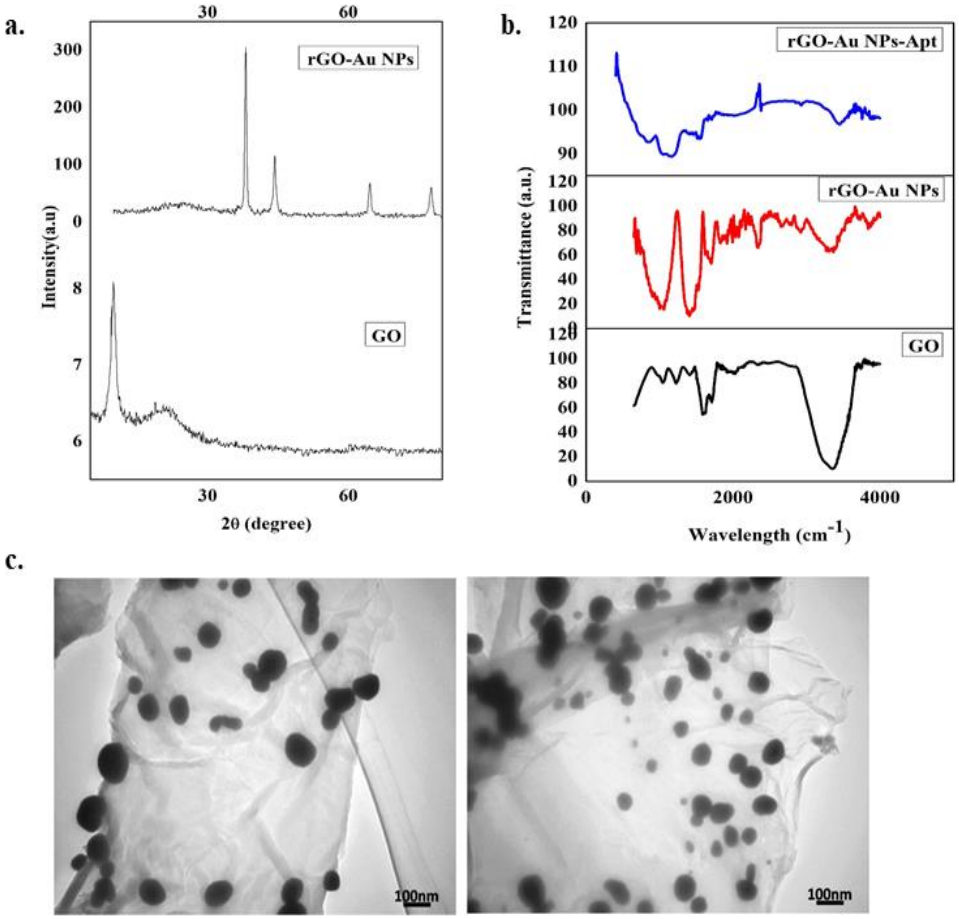

Figure 1 Characterization of synthesized nano-composites. (a) XRD spectra of GO and rGO-Au NPs. (b) FTIR spectra of GO, rGO-Au NPs, and rGO-Au NPs-Apt. (c)TEM of rGO-Au NPs.

3.2 Characterization of the modified electrode

To understand the electrochemical behavior of the modified electrode during the different stages of fabrication, cyclic voltammetry and electrochemical impedance spectroscopy for bare glassy carbon electrode, as well as modified electrodes were carried out. As shown in Figure 2 a. an increment in the peak current takes place after modifying the GCE with rGO-Au NPs, for the reason that gold nanoparticles maximize surface area and subsequently charge transfer. After the addition of nafion, the peak current decreases. This is the result of the attachment of nafion molecules to gold nanoparticles which leads to a slight drop of electron transfer around the electrode's surface. More significant decrease of the peak current was once displayed after the addition of aptamer and again after the addition of LPS biomolecules due to their hindrance effect on electrode's surface. Moreover, Figure 2 b. shows different EIS spectra of the modified electrodes, in which after dropping rGO-Au NPs, a considerable decrease of charge transfer resistance (Rct) can be observed. This is due to the positive effect of gold nanoparticles on electroactive surface of the electrode. Further, by adding nafion biomolecules on the surface of the modified electrode, electroactive surface of the electrode became smaller which leaded to a significant increment of Rct. By adding

aptamer and LPS biomolecules respectively on the modified electrode, the electroactive surface of the electrode as well as the charge transfer on this surface decreased even more and Rct became larger each time.

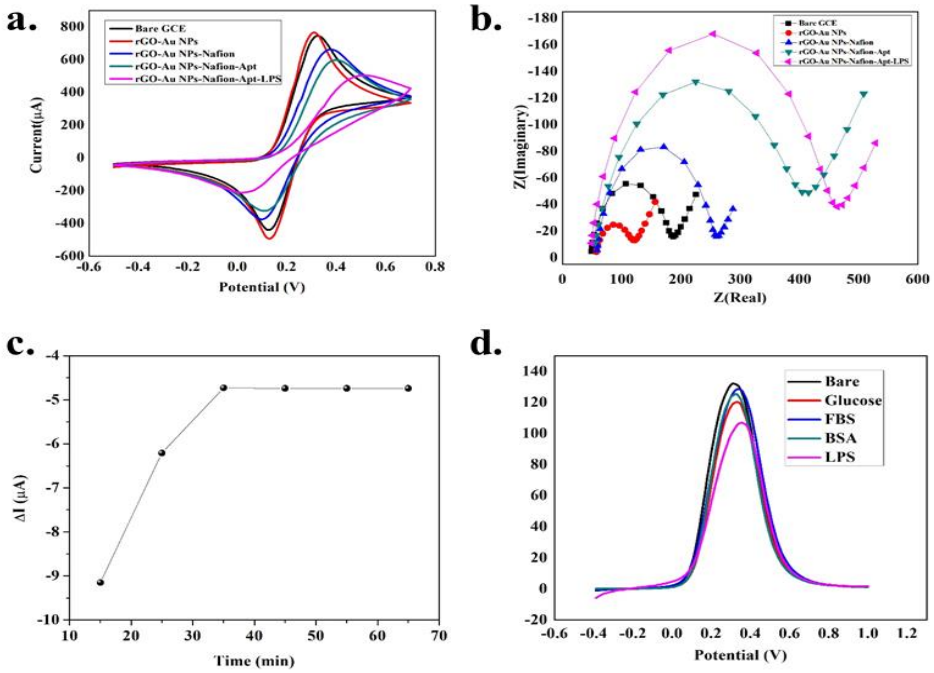

Figure 2 characterization of the modified electrode. (a) CV- and (b) EIS spectra of the modified electrode at different stages of the fabrication procedure. (c) Dependence of peak current and LPS incubation time (15,25, 35, 45, 55, 65 minutes). (d) the peak currents obtained from the SWV of the bare electrode and modified electrode after addition of different biomolecules.

The effect of LPS incubation time was investigated through SWV in K3Fe(CN)6 solution and the result of subtracting the peak current of the glassy carbon bare electrode from the obtained peak current related to each incubation time was depicted in Figure 2 c, which represents the relationship between incubation time and produced signals. It is clear that the peak currents decreased with the increment of the LPS incubation time, investigating that by giving adequate time, more endotoxin biomolecules occupied the aptamers on the electrode surface and made the electroactive surface of the electrode smaller, which was the main reason of slowing down the electron transfer and decline of the peak currents consequently. After 35 minutes the current value reached to a constant number, which shows the maximum attachments of LPS molecules to their specific aptamer molecules. As a result, 35 minutes was selected as the optimal LPS incubation time and the proper response time of the biosensor.

In order to assure that the fabricated biosensor is selective toward the LPS biomolecules, possible interfering biomolecules; fetal bovine serum (5 $ng.mL^{-1}$), bovine serum albumin (0.7$\mu g.mL^{-1}$), and glucose (110$mg.dl^{-1}$) were added separately to the modified electrode and the SWV peak currents of them in 2 mM K3Fe(CN)6 were obtained Figure 2 d. The results confirmed that the fabricated sensor is able to distinguish LPS (0.05 $ng.mL^{-1}$)

from other biomolecules, which is the direct result of the presence of a specific aptamer in the sensor's structure and the specificity of the applied aptamer toward endotoxin.

3.3 The square wave voltammetry signals and selectivity of electrode for real samples

Figure 3 shows the square wave voltammetry signals of the electrodes for normal, patient and Au-RGO/APT/NAF (or sensor base) groups. It is apparent that there is a reduction peak and a potential shift for patient group in comparison with normal one. As a result, ΔI between sensor base and patient group is higher than ΔI between sensor base and normal group.

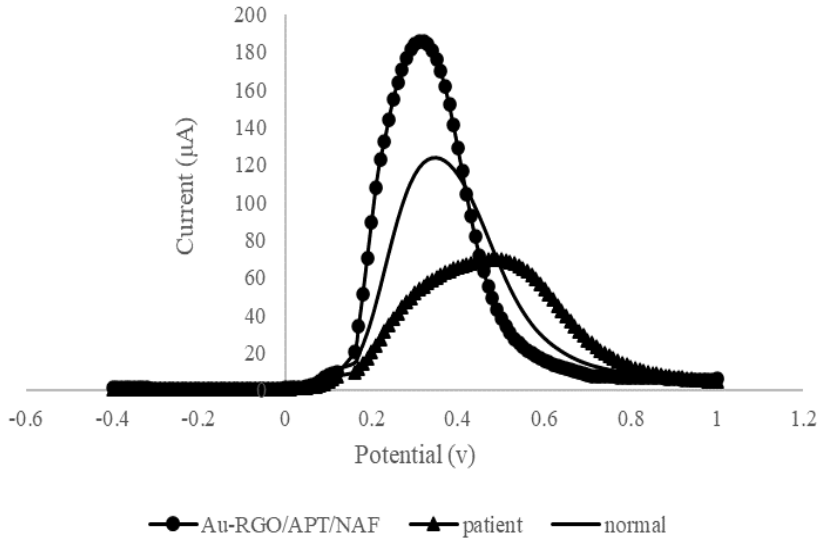

Figure 3: A square wave voltammetry signals of electrodes for normal, patient and Au-RGO/APT/NAF.

As shown in Figure 4, ΔI for patient groups are higher than normal groups. The range of ΔI can be considered for normal groups lower than 55 mA and for patient groups higher than 55 mA. Sensor response to normal groups can be due to the presence of interventional cases in real sample, because testing of real sample was done without dilution or removal of interventional cases.

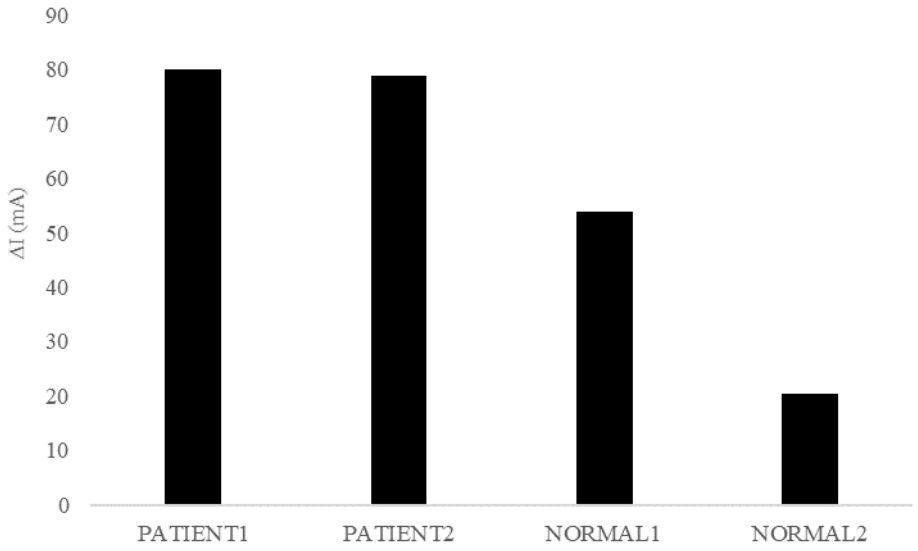

Figure 4: ΔI study of the aptasensor and comparison of response towards patient 1, patient 2, normal 1 and normal 2.

Table 1: Comparison some biosensors for detection of LPS

Detection method	Strategy	LOD	Linear range	Ref
Electrochemical (Su et al., 2012)	aptasensor	1 pg.mL−1	1–1000 pg.mL−1	
Electrochemical (Kim et al., 2012)	aptasensor	0.001 ng.mL−1	0.01 to 1 ng.mL−1	
Electrochemical (Su, Kim, et al., 2013)	aptasensor	0.005 ng. .mL−1	0. 01 to10.24 ng.mL−1	
Electrochemical (Su, Cho, et al., 2013)	gold nanoparticles/PEDOT	0.1 pg.mL−1	0.1–1000 pg.mL−1	
colorimetric (M. Miao et al., 2018)	anti-LPS aptamer	100 pg.mL−1	20 to 200 ng.mL−1	
Electrochemical	methylene blue aptasensor	0.2 fg.mL−1	0.001 to 0.01 pg.mL−1	present work

Conclusion

In conclusion, we have constructed an electrochemical label-free biosensor for the detection of trace levels of endotoxin. The magnificent properties of reduced graphene oxide including electrochemical activity, electrical conductivity, large surface area, ease of functionalization and biocompatibility along with benefit of integrating it with gold nanoparticles to improve its total surface area and electron transfer, made the rGO-Au NPs a great nanocomposite for fabricating an electrochemical biosensor. The selectivity of this biosensor toward LPS molecules is mainly due to the immobilized endotoxin-specific

aptamers on the rGO-Au NPs modified electrode. The final outstanding LOD and dynamic range of this aptasensor are 0.2 $fg.ml^{-1}$ and 0.001 to 0.01 $pg.ml^{-1}$ respectively. Additionally, real sample test proved that patient group has higher ΔI comparing with normal group.

This biosensor's ability in detecting endotoxin not only met the FDA required detection limit but also has shown to be better than most of the researches so far. The sensor exhibited excellent selectivity, stability, and sensitivity, along with being timesaving and effortless, which all suggest its potential to be used as an efficient LPS detection method in food-, environmental-, and pharmaceutical samples.

References

Akbari jonous, Z., Shayeh, J. S., Yazdian, F., Yadegari, A., Hashemi, M., & Omidi, M. (2019). An electrochemical biosensor for prostate cancer biomarker detection using graphene oxide–gold nanostructures. *Engineering in Life Sciences*. https://doi.org/10.1002/elsc.201800093

Bai, L., Chai, Y., Pu, X., & Yuan, R. (2014). A signal-on electrochemical aptasensor for ultrasensitive detection of endotoxin using three-way DNA junction-aided enzymatic recycling and graphene nanohybrid for amplification. *Nanoscale*. https://doi.org/10.1039/c3nr05930h

Das, A. P., Kumar, P. S., & Swain, S. (2014). Recent advances in biosensor based endotoxin detection. In *Biosensors and Bioelectronics*. https://doi.org/10.1016/j.bios.2013.07.020

Ding, X., Su, W., & Ding, X. (2015). Methods of Endotoxin Detection. In *Journal of Laboratory Automation*. https://doi.org/10.1177/2211068215572136

Doria, G., Conde, J., Veigas, B., Giestas, L., Almeida, C., Assunção, M., Rosa, J., & Baptista, P. V. (2012). Noble metal nanoparticles for biosensing applications. *Sensors*. https://doi.org/10.3390/s120201657

Erdem, A., Kerman, K., Meric, B., Akarca, U. S., & Ozsoz, M. (2000). Novel hybridization indicator methylene blue for the electrochemical detection of short DNA sequences related to the hepatitis B virus. *Analytica Chimica Acta*. https://doi.org/10.1016/S0003-2670(00)01058-8

Gao, W. (2015). The chemistry of graphene oxide. In *Graphene Oxide: Reduction Recipes, Spectroscopy, and Applications*. https://doi.org/10.1007/978-3-319-15500-5_3

Geim, A. K., & Novoselov, K. S. (2007). The rise of graphene. *Nature Materials*. https://doi.org/10.1038/nmat1849

Glauser, M. P., & Zanetti, G. (1991). Septic shock: pathogenesis. *The Lancet*, *338*(8769), 732–736.

Govindhan, M., Amiri, M., & Chen, A. (2015). Au nanoparticle/graphene nanocomposite as a platform for the sensitive detection of NADH in human urine. *Biosensors and Bioelectronics*, *66*, 474–480.

Ji, J., Pang, Y., Li, D., Huang, Z., Zhang, Z., Xue, N., Xu, Y., & Mu, X. (2020). An aptamer-based shear horizontal surface acoustic wave biosensor with a CVD-grown single-

layered graphene film for high-sensitivity detection of a label-free endotoxin. *Microsystems and Nanoengineering*. https://doi.org/10.1038/s41378-019-0118-6

Kim, S. E., Su, W., Cho, M., Lee, Y., & Choe, W. S. (2012). Harnessing aptamers for electrochemical detection of endotoxin. *Analytical Biochemistry*. https://doi.org/10.1016/j.ab.2012.02.016

Krittayavathananon, A., & Sawangphruk, M. (2017). Impedimetric sensor of ss-HSDNA/reduced graphene oxide aerogel electrode toward aflatoxin B1 detection: effects of redox mediator charges and hydrodynamic diffusion. *Analytical Chemistry*, *89*(24), 13283–13289.

Law, J. W. F., Mutalib, N. S. A., Chan, K. G., & Lee, L. H. (2014). Rapid metho ds for the detection of foodborne bacterial pathogens: Principles, applications, advantages and limitations. *Frontiers in Microbiology*. https://doi.org/10.3389/fmicb.2014.00770

Lee, C., Wei, X., Kysar, J. W., & Hone, J. (2008). Measurement of the elastic properties and intrinsic strength of monolayer graphene. *Science*. https://doi.org/10.1126/science.1157996

Liebers, V., Brüning, T., & Raulf-Heimsoth, M. (2006). Occupational endotoxin-exposure and possible health effects on humans. In *American Journal of Industrial Medicine*. https://doi.org/10.1002/ajim.20310

Luo, X., Morrin, A., Killard, A. J., & Smyth, M. R. (2006). Application of nanoparticles in electrochemical sensors and biosensors. In *Electroanalysis*. https://doi.org/10.1002/elan.200503415

Mairal, T., Cengiz Özalp, V., Lozano Sánchez, P., Mir, M., Katakis, I., & O'Sullivan, C. K. (2008). Aptamers: Molecular tools for analytical applications. *Analytical and Bioanalytical Chemistry*. https://doi.org/10.1007/s00216-007-1346-4

Miao, M., Tian, J., Luo, Y., Du, Z., Liang, Z., & Xu, W. (2018). Terminal deoxynucleotidyl transferase-induced DNAzyme nanowire sensor for colorimetric detection of lipopolysaccharides. *Sensors and Actuators, B: Chemical*. https://doi.org/10.1016/j.snb.2017.10.004

Miao, P. (2013). Electrochemical sensing strategies for the detection of endotoxin: A review. In *RSC Advances*. https://doi.org/10.1039/c3ra00047h

Park, C. Y., Jung, S. H., Bak, J. P., Lee, S. S., & Rhee, D. K. (2005). Comparison of the rabbit pyrogen test and Limulus amoebocyte lysate (LAL) assay for endotoxin in hepatitis B vaccines and the effect of aluminum hydroxide. *Biologicals*. https://doi.org/10.1016/j.biologicals.2005.04.002

Posha, B., Nambiar, S. R., & Sandhyarani, N. (2018). Gold atomic cluster mediated electrochemical aptasensor for the detection of lipopolysaccharide. *Biosensors and Bioelectronics*. https://doi.org/10.1016/j.bios.2017.10.030

Posha, B., & Sandhyarani, N. (2020). Highly sensitive endotoxin detection using a gold nanoparticle loaded layered molybdenum disulfide-polyacrylic acid nanocomposite. *The Analyst*. https://doi.org/10.1039/d0an00567c

Pourmadadi, M., Shayeh, J. S., Arjmand, S., Omidi, M., & Fatemi, F. (2020). An electrochemical sandwich immunosensor of vascular endothelial growth factor based on reduced graphene oxide/gold nanoparticle composites. *Microchemical Journal*, 105476.

Pourmadadi, M., Shayeh, J. S., Omidi, M., Yazdian, F., Alebouyeh, M., & Tayebi, L. (2019). A glassy carbon electrode modified with reduced graphene oxide and gold nanoparticles for electrochemical aptasensing of lipopolysaccharides from Escherichia coli bacteria. *Microchimica Acta*. https://doi.org/10.1007/s00604-019-3957-9

Sanguansak, Y., Srimuk, P., Krittayavathananon, A., Luanwuthi, S., Chinvipas, N., Chiochan, P., Khuntilo, J., Klunbud, P., Mungcharoen, T., & Sawangphruk, M. (2014). Permselective properties of graphene oxide and reduced graphene oxide electrodes. *Carbon*. https://doi.org/10.1016/j.carbon.2013.11.047

Schwartz, D. A., Thorne, P. S., Yagla, S. J., Burmeister, L. F., Olenchock, S. A., Watt, J. L., & Quinn, T. J. (1995). The role of endotoxin in grain dust-induced lung disease. *American Journal of Respiratory and Critical Care Medicine*. https://doi.org/10.1164/ajrccm.152.2.7633714

Shahriary, L., & Athawale, A. a. (2014). Graphene Oxide Synthesized by using Modified Hummers Approach. *International Journal of Renewable Energy and Environmental Engineering*.

Su, W., Cho, M., Nam, J., Choe, W., & Lee, Y. (2013). Aptamer-Assisted Gold Nanoparticles/PEDOT Platform for Ultrasensitive Detection of LPS. *Electroanalysis*, *25*(2), 380–386.

Su, W., Kim, S. E., Cho, M., Nam, J. Do, Choe, W. S., & Lee, Y. (2013). Selective detection of endotoxin using an impedance aptasensor with electrochemically deposited gold nanoparticles. *Innate Immunity*. https://doi.org/10.1177/1753425912465099

Su, W., Lin, M., Lee, H., Cho, M. S., Choe, W. S., & Lee, Y. (2012). Determination of endotoxin through an aptamer-based impedance biosensor. *Biosensors and Bioelectronics*. https://doi.org/10.1016/j.bios.2011.11.009

Vanegas, D. C., Rong, Y., Schwalb, N., Hills, K. D., Gomes, C., & McLamore, E. S. (2015). Rapid detection of listeria spp. using an internalin A aptasensor based on carbon-metal nanohybrid structures. *Smart Biomedical and Physiological Sensor Technology XII*. https://doi.org/10.1117/12.2177441

Wang, Z., Ping, Y., Fu, Q., & Pan, C. (2018). Preparation of Metal Nanoparticle Decorated Graphene Hybrid Composites: A Review. *MRS Advances*. https://doi.org/10.1557/adv.2018.30

Wu, Y., & Chai, H. (2017). Development of an electrochemical biosensor for rapid detection of foodborne pathogenic Bacteria. *Int. J. Electrochem. Sci*, *12*, 4291–4300.

Xu, X., Bao, Z., Zhou, G., Zeng, H., & Hu, J. (2016). Enriching Photoelectrons via Three Transition Channels in Amino-Conjugated Carbon Quantum Dots to Boost Photocatalytic Hydrogen Generation. *ACS Applied Materials and Interfaces*. https://doi.org/10.1021/acsami.6b02961

Yuan, Y., Li, L., Zhao, M., Zhou, J., Chen, Z., & Bai, L. (2019). An aptamer based voltammetric biosensor for endotoxins using a functionalized graphene and molybdenum disulfide composite as a new nanocarrier. *Analyst*. https://doi.org/10.1039/c8an02139b

Zejli, H., Goud, K. Y., & Marty, J. L. (2019). An electrochemical aptasensor based on polythiophene-3-carboxylic acid assisted methylene blue for aflatoxin B1 detection. In *Sensing and Bio-Sensing Research*. https://doi.org/10.1016/j.sbsr.2019.100290

Zhang, Z., Yu, H. W., Wan, G. C., Jiang, J. H., Wang, N., Liu, Z. Y., Chang, D., & Pan, H. Z. (2017). A label-free electrochemical biosensor based on a reduced graphene oxide and indole-5-carboxylic acid nanocomposite for the detection of klebsiella pneumoniae. *Journal of AOAC International*. https://doi.org/10.5740/jaoacint.16-0251

Zhao, Y., Cong, L., Jaber, V., & Lukiw, W. J. (2017). Microbiome-derived lipopolysaccharide enriched in the perinuclear region of Alzheimer's disease brain. *Frontiers in Immunology*. https://doi.org/10.3389/fimmu.2017.01064

Zuzuarregui, A., Souto, D., Pérez-Lorenzo, E., Arizti, F., Sánchez-Gómez, S., Martínez De Tejada, G., Brandenburg, K., Arana, S., & Mujika, M. (2015). Novel integrated and portable endotoxin detection system based on an electrochemical biosensor. *Analyst*. https://doi.org/10.1039/c4an01324g